Electronic Supplementary Materials

Oxygen reduction reaction (ORR) in alkaline solution catalysed by an atomically precise catalyst based on a Pd(II) complex supported on multi walled carbon nanotubes (MWCNTs). Electrochemical and structural considerations.

Valeria Monini, Marco Bonechi, Carla Bazzicalupi, Antonio Bianchi, Pietro Gentilesca, Walter Giurlani, Massimo Innocenti, Arianna Meoli, Giammarco Maria Romano and Matteo Savastano

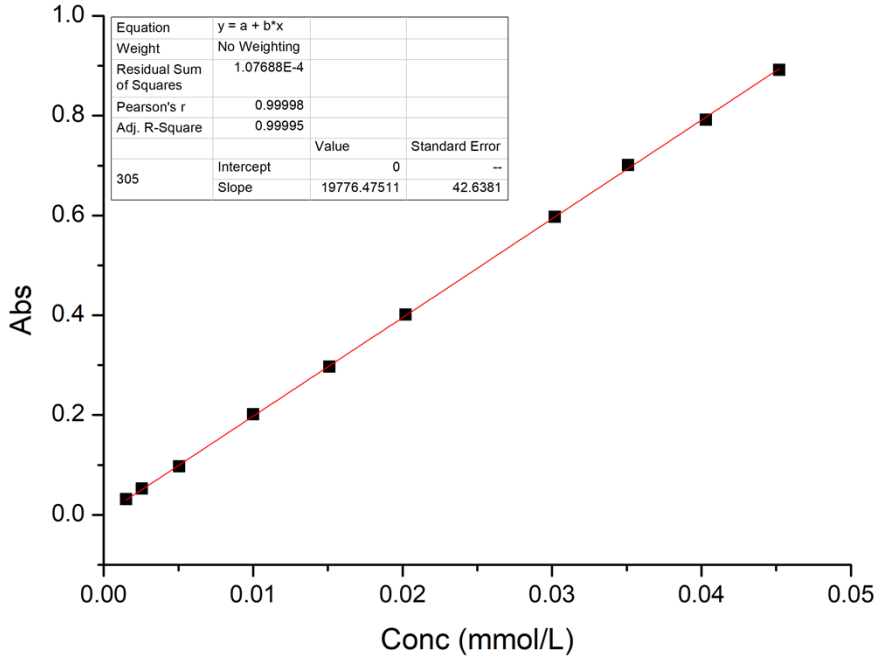

Figure S1. Experimental calibration curve for the determination of H_2L concentration in solution obtained with the absorbance at 305 nm. Determined molar absorbance ε = 19776(43) $L \cdot mol^{-1} \cdot cm^{-1}$

Table S1. Crystal data and refinement parameters for $(H_5L)(ClO_4)_3{\cdot}2H_2O$ (a), $(H_3L)(H_4L)(ClO_4)_3{\cdot}11H_2O$ (b), $[Cu(H_2L)(H_2O)](ClO_4)_2{\cdot}10.46H_2O$ (c), $[Cu(H_2L)Cl]Cl{\cdot}3H_2O$ (d) and $[Pd(\mathbf{1})]Cl_2{\cdot}4H_2O$ (e)

	(a)	(b)	(c)	(d)	(e)
Empirical formula	$C_{24}H_{49}Cl_3N_{14}O_{18}$	$C_{48}H_{109}Cl_3N_{28}O_{31}$	$C_{24}H_{64.92}Cl_2CuN_{14}O_{23.46}$	$C_{24}H_{48}Cl_2CuN_{14}O_7$	$C_{56}H_{96}Cl_4N_{12}O_{16}Pd_2S_4$
Formula weight	928.12	1680.98	1059.62	779.20	1676.28
Temperature (K)	100(2)	100(2)	100(2)	100(2)	100(2)
Crystal system	Triclinic	Monoclinic	Triclinic	Triclinic	Triclinic
space group	*P* -1	*C* 2/c	*P* -1	*P* -1	*P* -1
a (Å)	12.5685(3)	36.1345(14)	9.5546(3)	10.7356(14)	9.8464(3)
b (Å)	12.8470(3)	8.3617(3)	12.9018(4)	13.2246(16)	18.5362(7)
c (Å)	12.9863(3)	25.1795(10)	19.4955(6)	13.6742(16)	21.2826(8)
α (°)	74.359(1)	90	74.443(2)	62.602(4)	97.607(2)
β (°)	86.816(1)	92.056(3)	79.300(2)	75.161(5)	99.894(2)
γ (°)	76.531(1)	90	76.145(2)	80.721(5)	100.807(2)
Volume (Å^3)	1963.62(8)	7603.0(5)	2228.81(12)	1664.0(4)	3704.0(2)
Z	2	4	2	2	2
Independent reflections / R(int)	7214/0.0747	8184/0.0845	7832/0.0703	10201/0.0913	10301/0.0946
μ (mm^{-1})	2.934 (Cu-kα)	1.966 (Cu-kα)	2.665 (Cu-kα)	0.883 (Mo-kα)	6.872 (Cu-kα)
R indices [I>2σ(I)][a]	R1 = 0.0904	R1 = 0.0793	R1 = 0.0602	R1 = 0.0757	R1 = 0.0874
	wR2 = 0.2432	wR2 = 0.2294	wR2 = 0.1727	wR2 = 0.1867	wR2 = 0.2264
R indices (all data)[a]	R1 = 0.1051	R1 = 0.0869	R1 = 0.0659	R1 = 0.0998	R1 = 0.1327
	wR2 = 0.2577	wR2 = 0.2401	wR2 = 0.1798	wR2 = 0.2069	wR2 = 0.2643

[a] $R1 = \Sigma \, || Fo| - |Fc|| / \Sigma \, |Fo|$; $wR2 = [\Sigma \, w(Fo^2 - Fc^2)^2 / \Sigma \, wF$

Table S2. Selected bond distances (Å) and angles (deg) for metal coordination environment in $[Cu(H_2L)(H_2O)](ClO_4)_2 \cdot 10.46H_2O$ and (d) $[Cu(H_2L)Cl]Cl \cdot 3H_2O$

$[Cu(H_2L)(H_2O)](ClO_4)_2 \cdot 10.46H_2O$		**$[Cu(H_2L)Cl]Cl \cdot 3H_2O$**	
Cu - OW1	2.130(3)	Cu - Cl1	2.411(1)
Cu - N4	2.030(3)	Cu - N1	2.075(4)
Cu - N2	2.041(3)	Cu - N3	2.072(4)
Cu - N1	2.042(3)	Cu - N2	2.042(5)
Cu - N3	2.048(3)	Cu - N4	2.031(5)
OW1 - Cu - N4	103.9(1)	Cl1 - Cu - N1	106.3(1)
OW1 - Cu - N2	102.6(1)	Cl1 - Cu - N3	104.5(1)
OW1 - Cu - N1	104.5(1)	Cl1 - Cu - N2	105.3(1)
OW1 - Cu - N3	104.4(1)	Cl1 - Cu - N4	105.1(1)
N4 - Cu - N2	153.5(1)	N1 - Cu - N3	149.2(1)
N4 - Cu - N1	86.6(1)	N1 - Cu - N2	85.2(2)
N4 - Cu - N3	86.6(1)	N1 - Cu - N4	85.7(1)
N2 - Cu - N1	86.8(1)	N3 - Cu - N2	87.0(2)
N2 - Cu - N3	86.9(1)	N3 - Cu - N4	86.2(2)
N1 - Cu - N3	151.1(1)	N2 - Cu - N4	149.6(2)

Table S3. Selected bond distances (Å) and angles (deg) for metal coordination environment in $[Pd(\mathbf{1})]Cl_2 \cdot 4H_2O$

Mol A		**Mol B**	
Pd1 - N2	2.038(8)	Pd2 - N7	2.04(1)
Pd1 - N3	2.06(1)	Pd2 - N8	2.036(9)
Pd1 - N1	2.05(1)	Pd2 - N10	2.058(9)
Pd1 - N4	2.037(9)	Pd2 - N9	2.03(1)
Pd1···N6	3.09(1)	Pd2···N11	3.00(1)
N2 - Pd1 - N3	88.1(4)	N7 - Pd2 - N8	88.1(4)
N2 - Pd1 - N1	87.2(4)	N7 - Pd2 - N10	87.7(4)
N2 - Pd1 - N4	158.3(4)	N7 - Pd2 - N9	159.6(4)
N3 - Pd1 - N1	158.5(4)	N8 - Pd2 - N10	157.9(4)
N3 - Pd1 - N4	88.3(4)	N8 - Pd2 - N9	88.1(4)
N1 - Pd1 - N4	88.4(4)	N10 - Pd2 - N9	88.3(4)

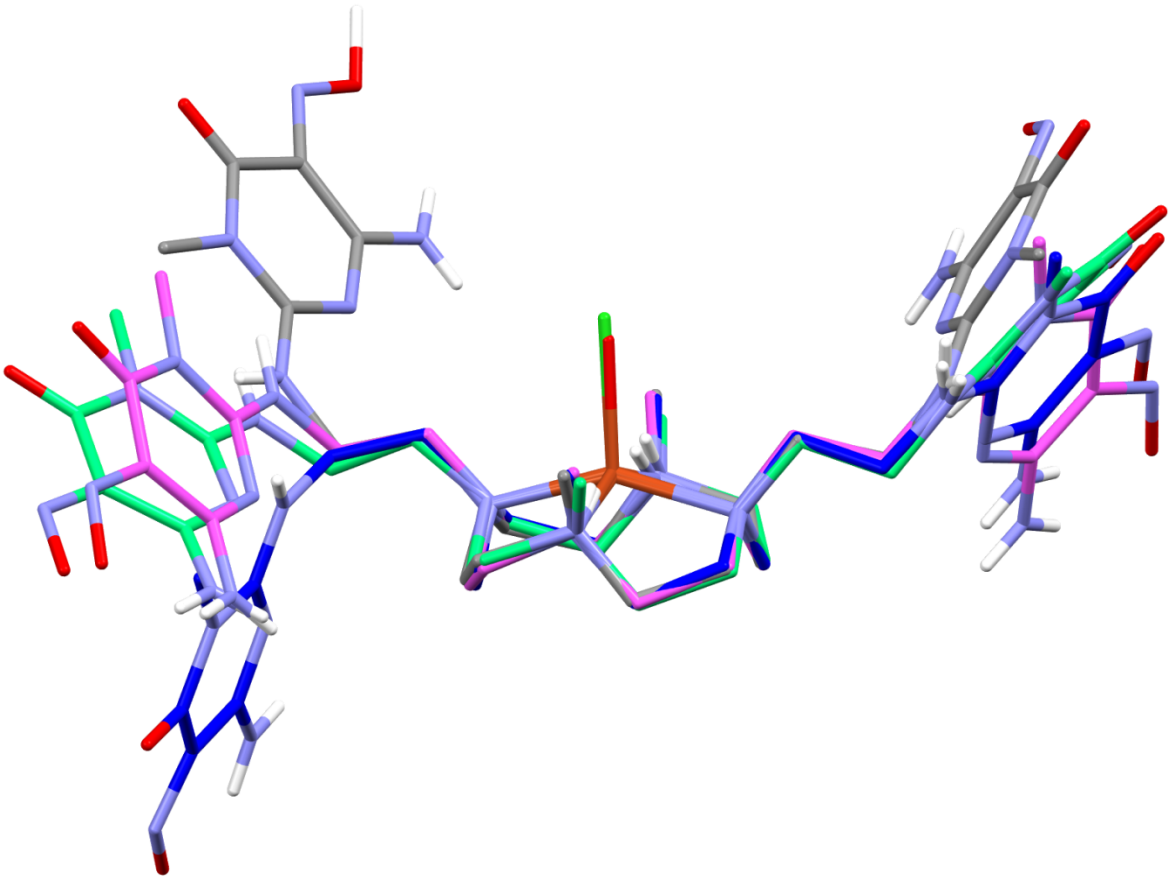

Figure S2. Superposition of H_2L ligands in the crystal structures of $(H_5L)(ClO_4)_3 \cdot 2H_2O$ (gray), $(H_3L)(H_4L)(ClO_4)_3 \cdot 11H_2O$ (green – only the prevalent conformer is shown), $[Cu(H_2L)(H_2O)]$ $)(ClO_4)_2 \cdot 10.46H_2O$ (pink) and $[Cu(H_2L)Cl]Cl \cdot 3H_2O$) (blue).

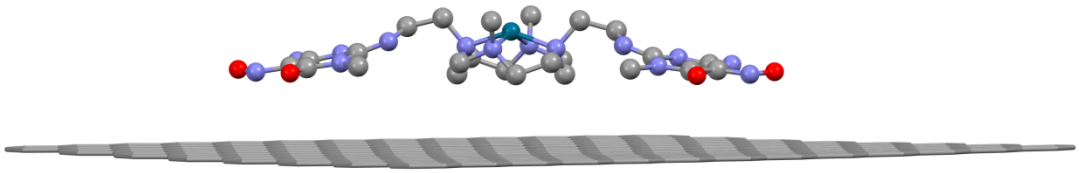

Figure S3. Preliminary results from molecular dynamics simulation (empirical forcefield method) for the $[Pd(H_2L)]^{2+}$ cation interacting with a graphene slice as a model for the MWCNT (HyperChem(TM) Professional 8, Hypercube, Inc., 1115 NW 4th Street, Gainesville, Florida 32601, USA).

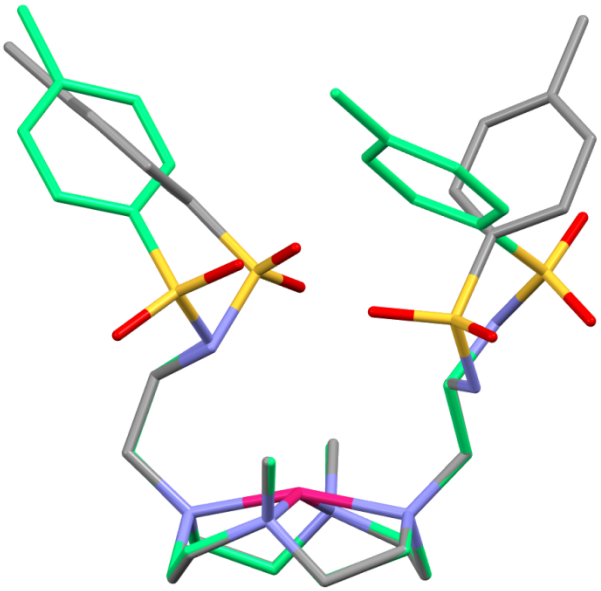

Figure S4. Superimposition of the two not symmetry equivalent $[Pd(\mathbf{1})]^{2+}$ complexes in the $[Pd(\mathbf{1})]Cl_2 \cdot 4H_2O$ crystal structure.

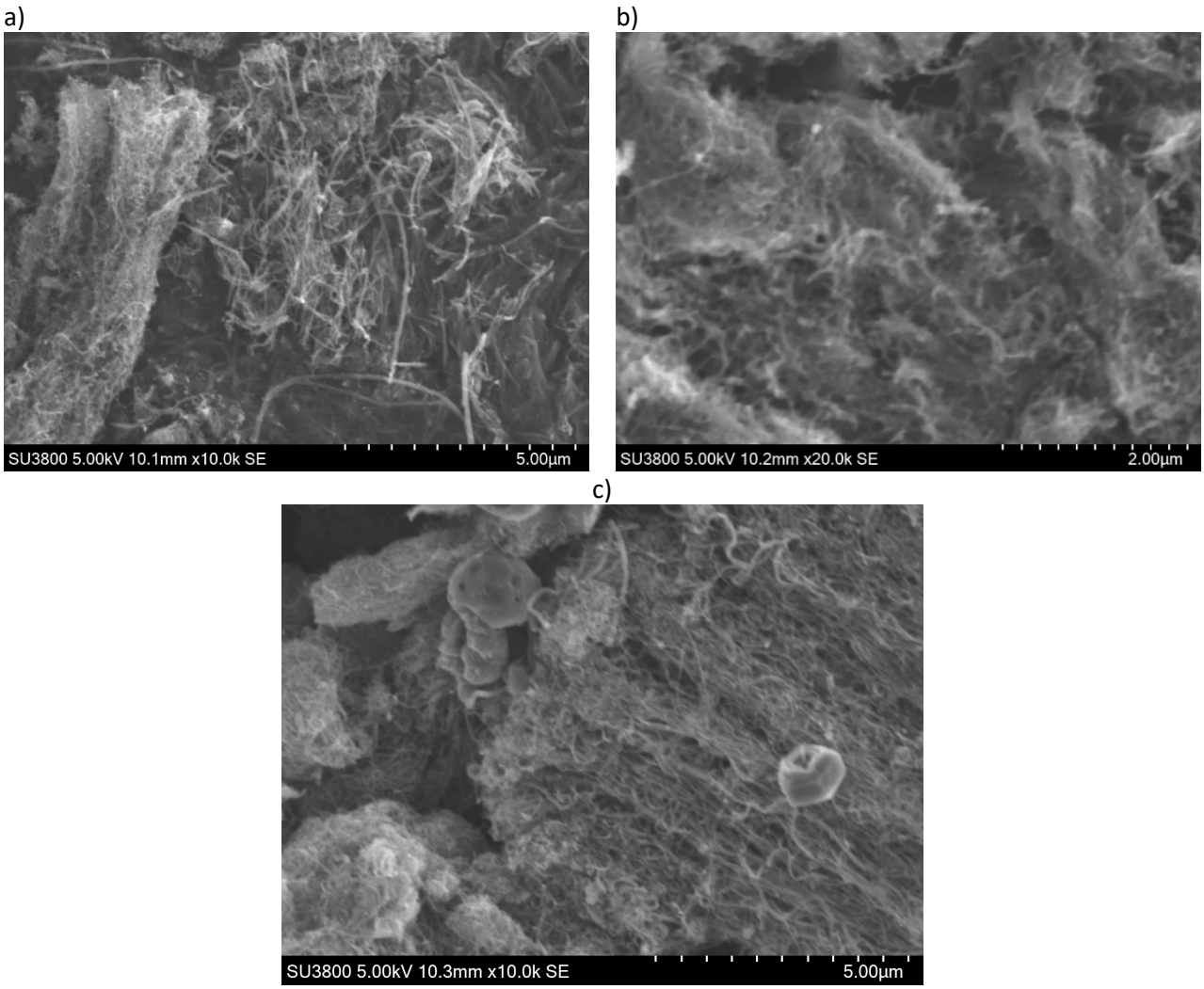

Figure S5. SEM micrographs showing a) MWCNT before functionalisation, b) MWCNT-L, c) as-prepared MWCNT-LPd. Recorded on a Hitachi SU3800 instrument.

a)

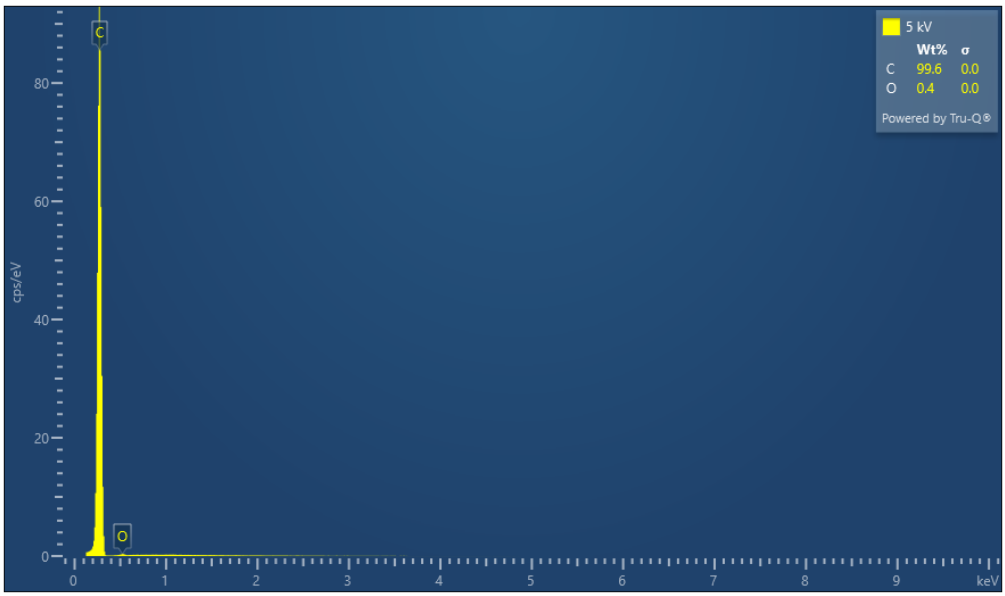

b)

c)

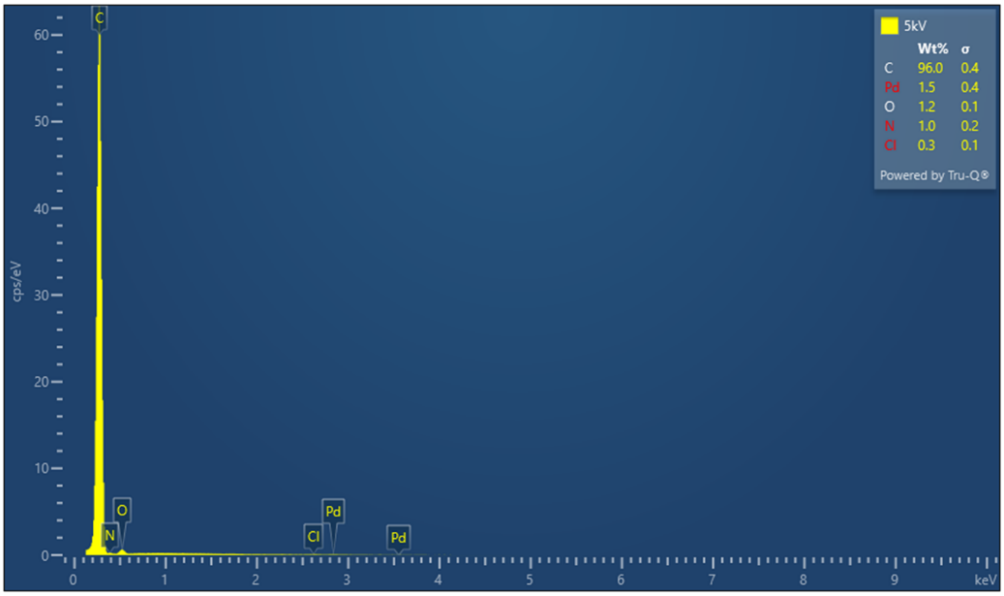

Figure S6. SEM-EDS analysis. Spectra and % m/m of a) MWCNT before functionalisation, b) MWCNT-L , c) as-prepared MWCNT-LPd.

a)

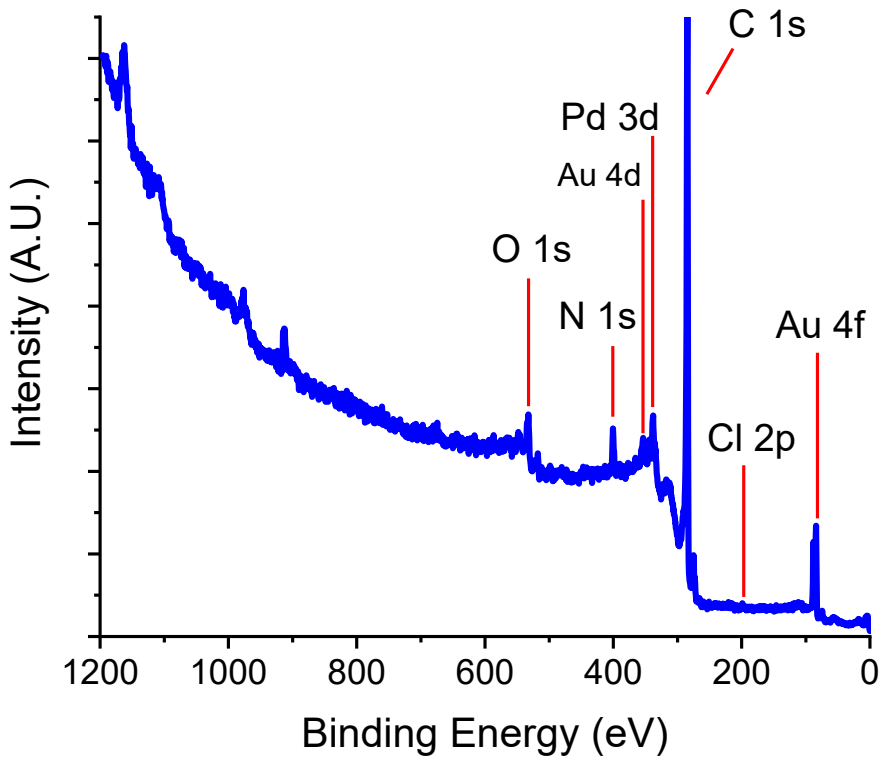

b)

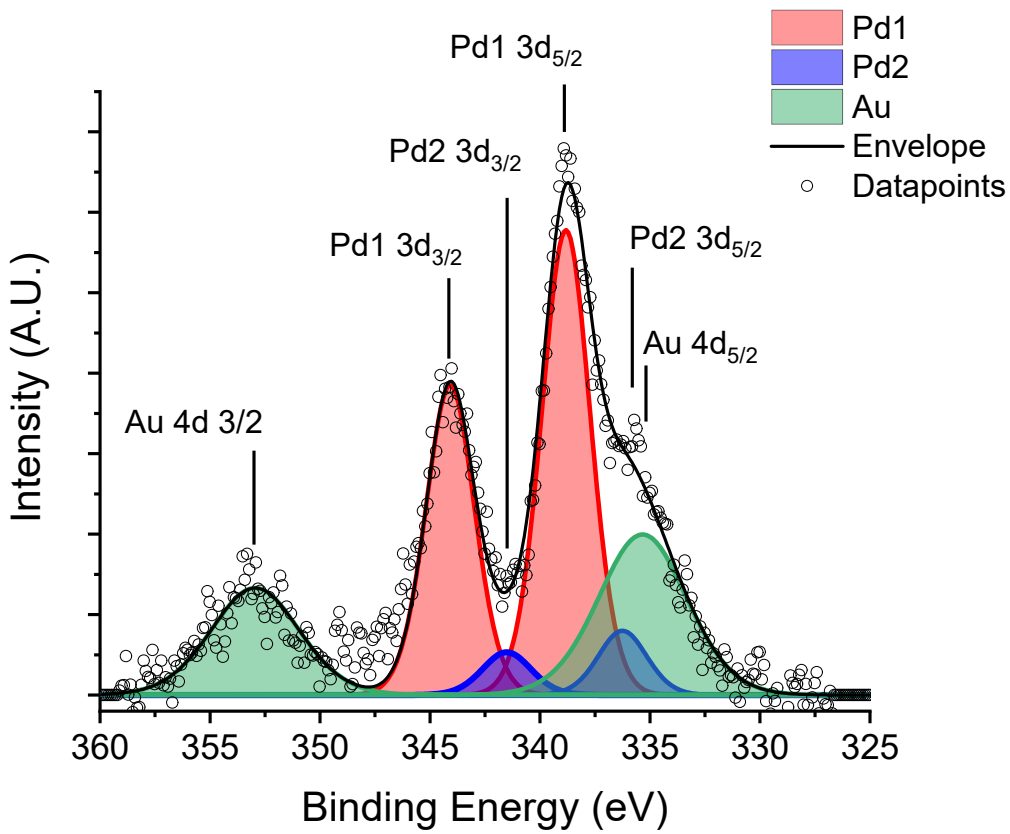

Figure S7. XPS Analysis of MWCNT-LPd catalyst. a) XPS survey spectra, b) high resolution XPS spectra in the Pd 3d region deconvoluted into two main components named Pd1 (+2 oxidation state, red colour) and Pd2 (PdO/C, blue colour). Black line: global fit of experimental data; black dot: experimental data, green line corresponds to Au signals from the Au sample holder.

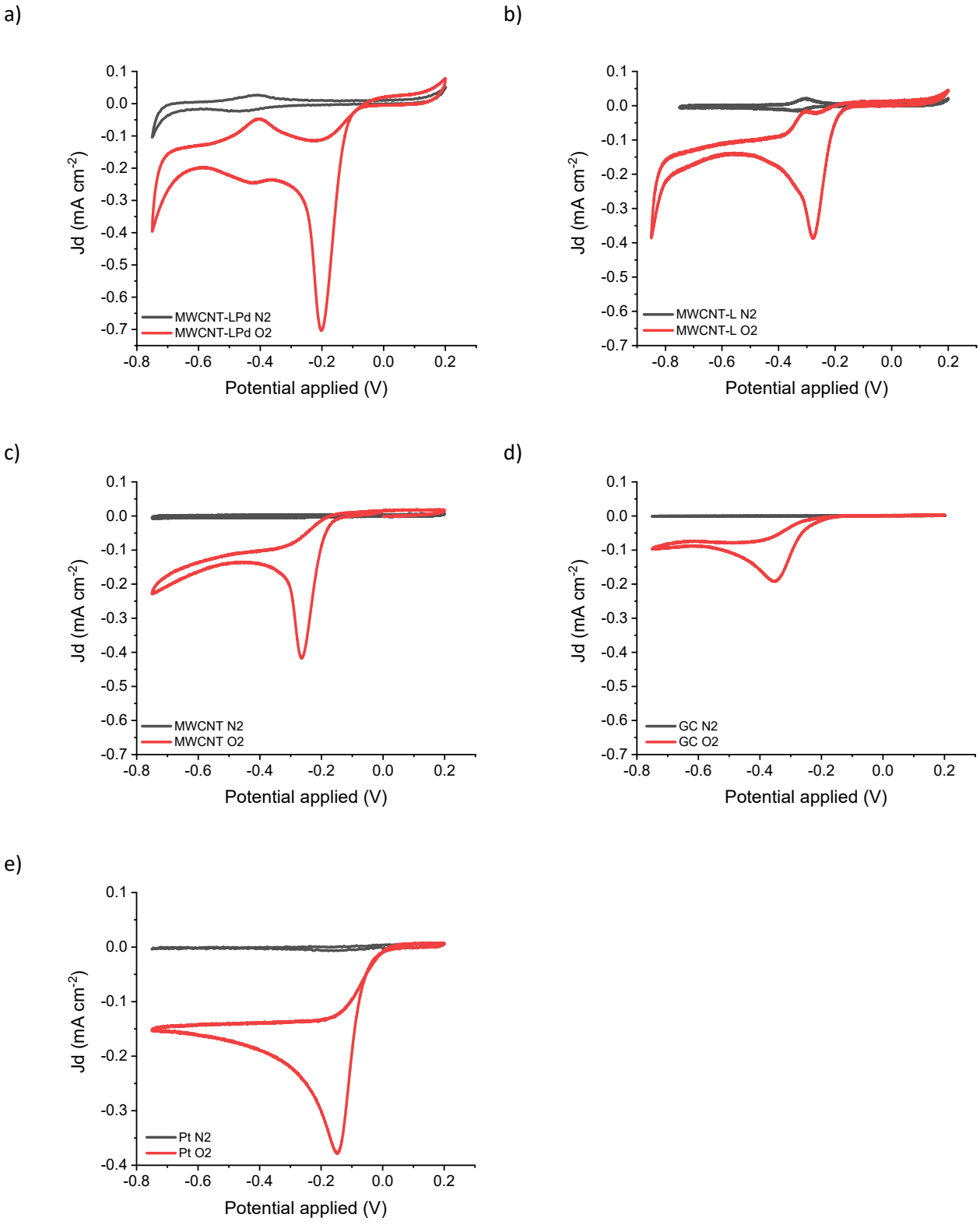

Figure S8. Cyclic voltammetry of modified electrodes in KOH 0.1M solution saturated with N_2 (black line) and O_2 (red line) between +0.2 and −0.75 V at a potential scan rate of 5 mVs^{-1} a) MWCNT-LPd, b) MWCNT-L, c) MWCNT, d) benchmark GC electrode, e) benchmark Pt electrode.

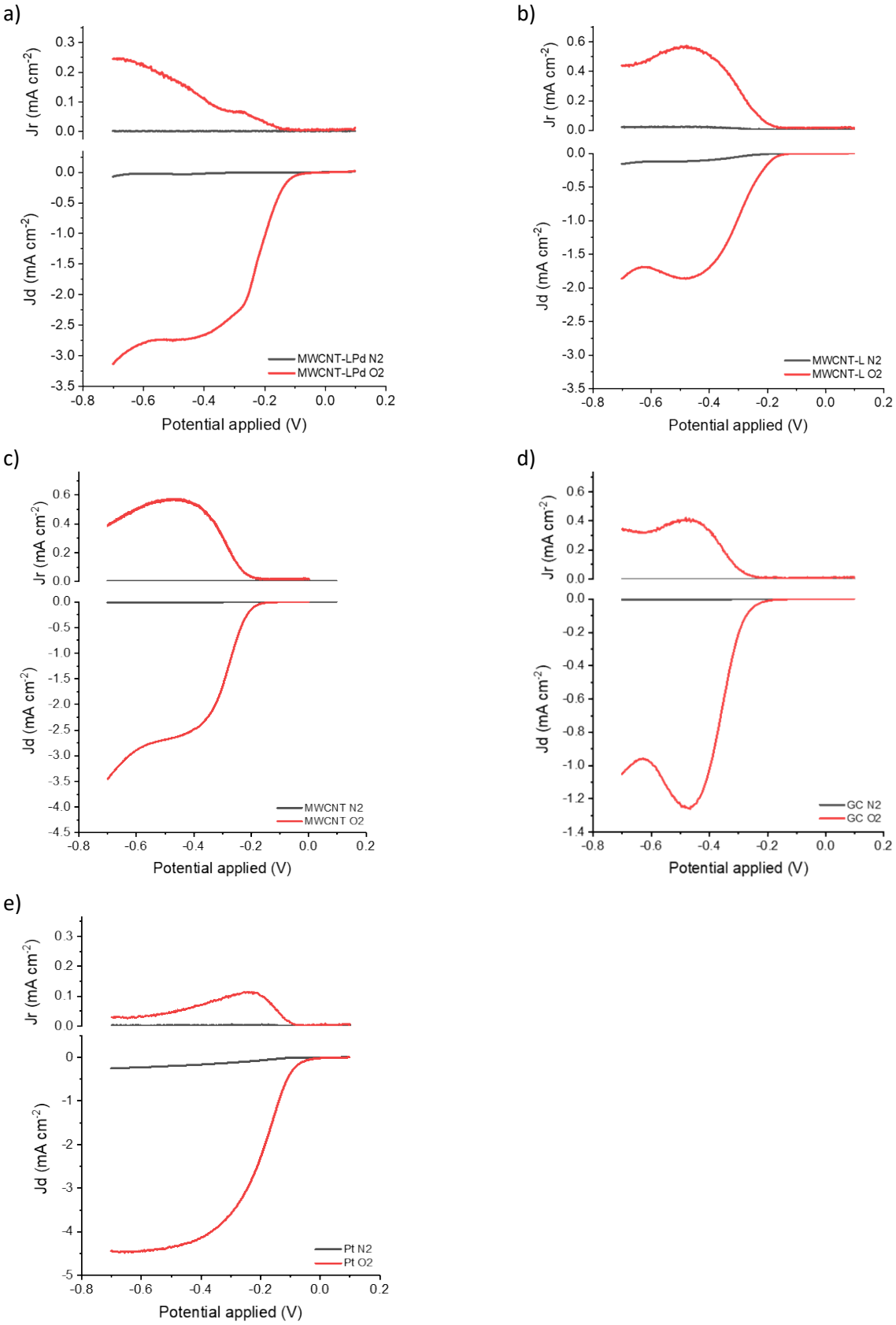

Figure S9. LSV ring and disk current density, 1600 rpm rotation rate, 5 mVs^{-1} scan rate, in KOH 0.1 M N_2 and O_2 saturated solution. a) MWCNT-LPd, b) MWCNT-L, c) MWCNT, d) benchmark GC electrode, e) benchmark Pt electrode.

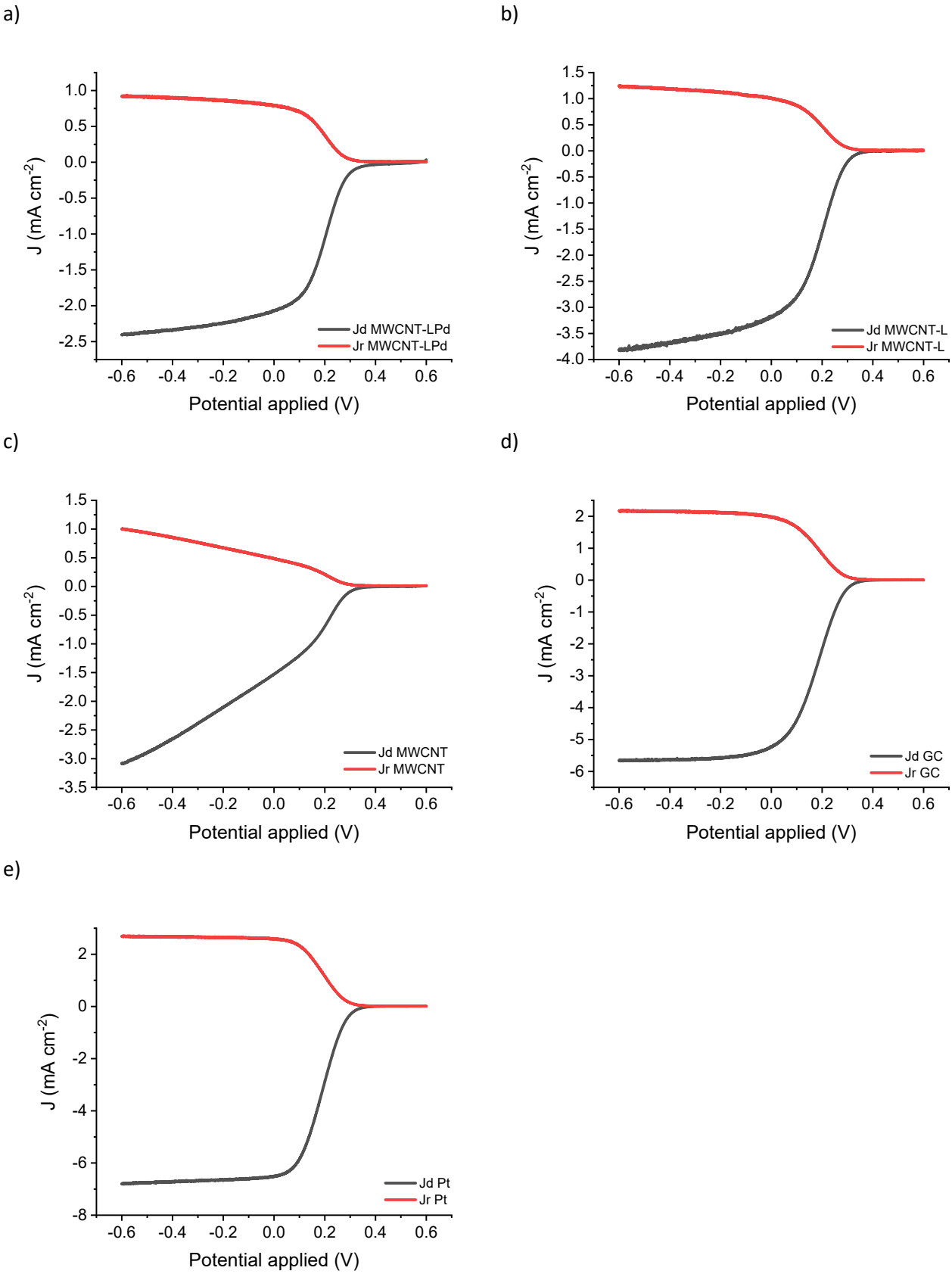

Figure S10. LSV ring and disk current density, 1600 rpm rotation rate, 5 mVs^{-1} scan rate, in $K_3Fe(CN)_6$ 1mM, KCl 0.1 M O_2 free solution. a) MWCNT-LPd (N = 0.38), b) MWCNT-L (N = 0.32), c) MWCNT (N = 0.32), d) benchmark GC electrode (N = 0.38), e) benchmark Pt electrode (N = 0.38).

a)

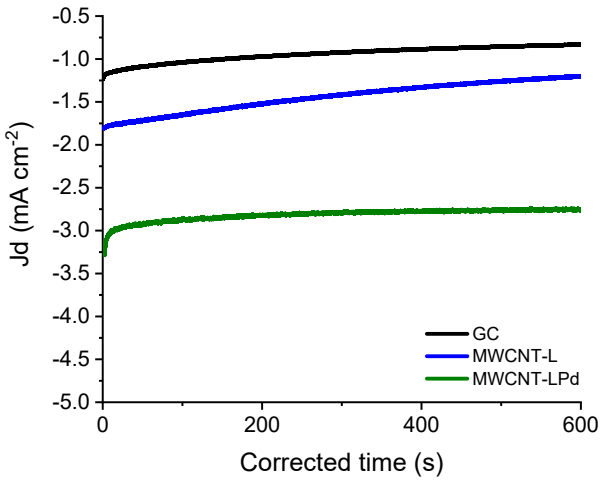

b)

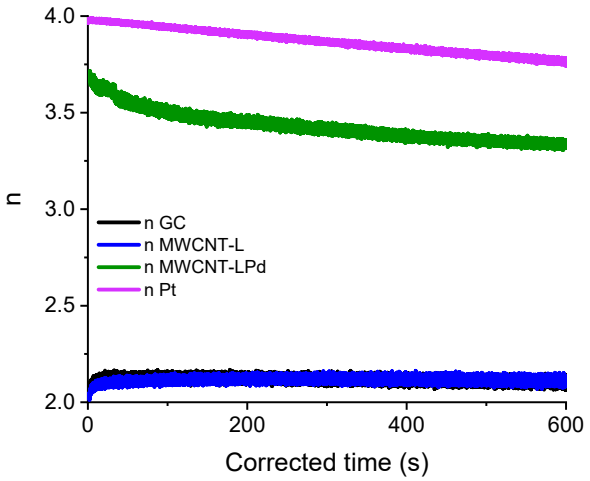

Figure S11. Short-time stability test (galvanostatic RRDE experiment) of ORR electrocatalytic performance. Disk potential −0.60 V, ring potential +0.50 V, 1600 rpm rotation rate in KOH 0.1 M O_2 saturated solution. a) disk currents density of modified GC electrodes and benchmark electrodes b) number of exchanged electrons per O_2 molecule over time.